

# Suppressing epidemic spreading by risk-averse migration in dynamical networks

Han-Xin Yang<sup>1,\*</sup>, Ming Tang<sup>2,3</sup>, and Zhen Wang<sup>4</sup>

<sup>1</sup>*Department of Physics, Fuzhou University, Fuzhou 350116, China*

<sup>2</sup>*School of Information Science Technology, East China Normal University, Shanghai 200062, China*

<sup>3</sup>*Big data research center, University of Electronic Science and Technology of China, Chengdu 611731, China*

<sup>4</sup>*Center for OPTical IMagery Analysis and Learning (OPTIMAL),  
Northwestern Polytechnical University, Xi'an 710072, Shaanxi, China*

(Dated: March 15, 2022)

In this paper, we study the interplay between individual behaviors and epidemic spreading in a dynamical network. We distribute agents on a square-shaped region with periodic boundary conditions. Every agent is regarded as a node of the network and a wireless link is established between two agents if their geographical distance is less than a certain radius. At each time, every agent assesses the epidemic situation and make decisions on whether it should stay in or leave its current place. An agent will leave its current place with a speed if the number of infected neighbors reaches or exceeds a critical value  $E$ . Owing to the movement of agents, the network's structure is dynamical. Interestingly, we find that there exists an optimal value of  $E$  leading to the maximum epidemic threshold. This means that epidemic spreading can be effectively controlled by risk-averse migration. Besides, we find that the epidemic threshold increases as the recovering rate increases, decreases as the contact radius increases, and is maximized by an optimal moving speed. Our findings offer a deeper understanding of epidemic spreading in dynamical networks.

PACS numbers: 89.75.Hc, 87.19.X-

Keywords: Epidemic spreading; Migration; Risk; Dynamical networks

## I. INTRODUCTION

The study of epidemic spreading in complex networks has received increasing attention since the 21st Century [1]. In the original model, individuals in the network are set to be “passive” nodes awaiting to be infected. However, in reality, when individuals become aware of the potential disease, they would take preventive measures (e.g., avoiding contact with infected individuals, wearing protective masks, or vaccination) to protect themselves.

The interplay between individual behaviors and epidemic dynamics in complex networks has attracted growing interest in recent years [2–12]. For example, Gross *et al.* proposed an adaptive epidemic dynamical model, in which the susceptible breaks the link to the infected and forms a new link to another randomly selected susceptible, and the adaptive system displayed assortative degree correlation, oscillations, hysteresis, and first order transitions [13]. Funk *et al.* studied the impacts of awareness spread on both epidemic threshold and prevalence, and they found that, in a well-mixed population, spread of awareness can reduce the prevalence of epidemic but does not tend to affect the epidemic threshold [14]. Granell *et al.* investigated the interplay between awareness and epidemic spreading in multiplex networks, and revealed the existence of a metacritical point at which the critical onset of the epidemics starts depending on the reaching of the awareness process [15]. Wang *et al.* studied the asymmetrically interacting spreading dynamics based on a two susceptible-infected-recovered processes coupled model in multiplex networks, and found that the propagation of information can lead to the increase of the epidemic threshold [16]. Xia *et al.* introduced a Susceptible-Infected-Removed model with infection delay and propagation vector [17]. They found that both of the factors can markedly reduce the critical threshold of disease infection and accelerate the dynamical processes of epidemic spreading. Furthermore, they studied effects of delayed recovery and nonuniform transmission on the spreading of diseases [18].

It has been known that in real-life situations, when epidemics outbreaks, individuals often escape from the infected areas and migrate to other regions. Based on such fact, we propose a risk-averse migration model, in which each individual assesses the epidemic situation and make decisions on whether it should stay in or leave its current place. We assume that an individual will migrate to other places if the number of infected neighbors reaches or exceeds a critical value of  $E$  (we call it as the risk threshold). The larger value of  $E$  means that individuals are able to endure a greater risk of being infected. Interestingly, we find a nonmonotonic behavior in that the epidemic threshold can be

---

\*Electronic address: yanghanxin001@163.com

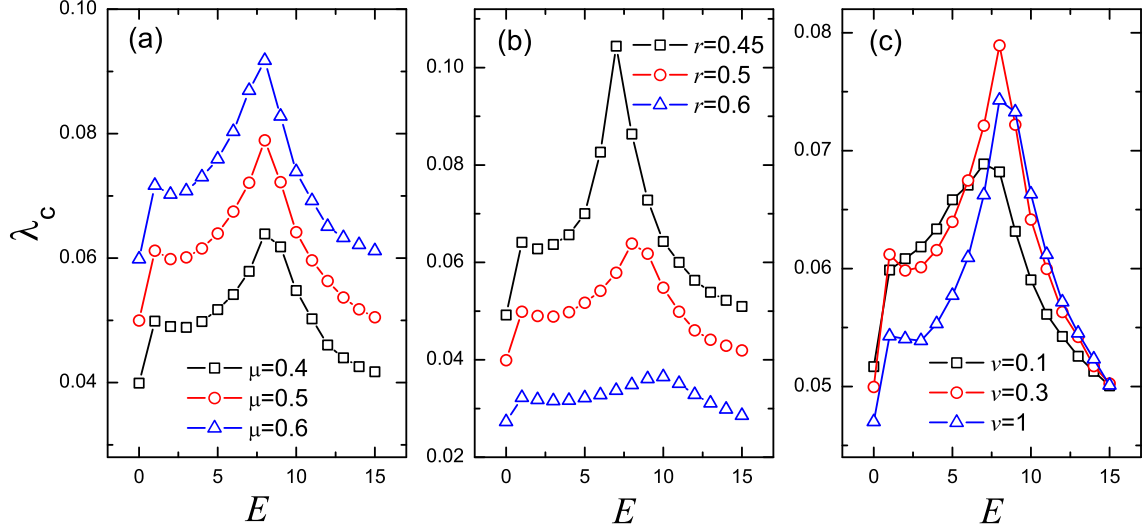


FIG. 1: (Color online) (a) The epidemic threshold  $\lambda_c$  as a function of the risk threshold  $E$  for different values of the recovering rate  $\mu$ . The contact radius  $r = 0.5$  and the moving speed  $v = 0.3$ . (b) The epidemic threshold  $\lambda_c$  as a function of  $E$  for different values of the contact radius  $r$ . The recovering rate  $\mu = 0.4$  and the moving speed  $v = 0.3$ . (c) The epidemic threshold  $\lambda_c$  as a function of  $E$  for different values of the moving speed  $v$ . The recovering rate  $\mu = 0.5$  and the contact radius  $r = 0.5$ . Each data point is result of averaging over 100 random realizations.

maximized at a moderate value of  $E$ . This means that we can control the outbreak of epidemic by a proper choice of the risk-averse migration.

## II. MODEL

In our model,  $N$  agents are distributed on a square-shaped cell of size  $L$  with periodic boundary conditions. We utilize the standard susceptible-infected-susceptible (SIS) dynamical process for modeling epidemic spreading. Two agents can contact with each other if their distance is less than  $r$  (which we call it as the contact radius). An initial fraction of agents  $\rho_0$  is set to be infected (we set  $\rho_0 = 0.1$  in numerical experiments). At each time step, each susceptible agent is infected with probability  $\lambda$  if it contacts with an infected agent. At the same time, infected agents are cured and become again susceptible with probability  $\mu$ .

The initial positions of agents are randomly distributed. After each time step, each agent  $i$  decides whether to stay in or leave its current position. If the number of infected agents within the contact radius is less than a threshold  $E$ , an agent does not move. Otherwise, agent  $i$  moves and updates its position according to:

$$x_i(t+1) = x_i(t) + v \cos \theta_i(t), \quad (1)$$

$$y_i(t+1) = y_i(t) + v \sin \theta_i(t), \quad (2)$$

where  $x_i(t)$  and  $y_i(t)$  are the coordinates of agent  $i$  at time  $t$ ,  $v$  is the moving speed, and  $\theta_i(t)$  is a random variable chosen from the interval  $[-\pi, \pi]$ .

In the present model, we consider the local information-based awareness, that is, an individual only knows the states of its neighbors. Due to the limitation of local information, a migrant may not wisely choose the new destination. Thus, the moving directions are randomly set. Note that for  $E = 0$ , all agents move at each time step. For a sufficiently large value of  $E$ , all agents stay still.

## III. RESULTS AND DISCUSSIONS

In all the following simulations, we set the total number of agents  $N = 1500$  and the size of the square region  $L = 10$  if there is no special mention.

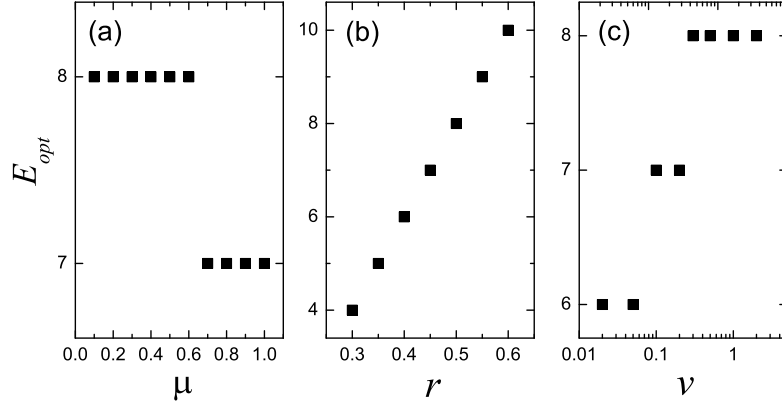


FIG. 2: (a) The optimal value of the risk threshold  $E$ ,  $E_{opt}$ , as a function of the recovering rate  $\mu$ . The contact radius  $r = 0.5$  and the moving speed  $v = 0.3$ . (b) The dependence of  $E_{opt}$  on the contact radius  $r$ . The recovering rate  $\mu = 0.4$  and the moving speed  $v = 0.3$ . (c) The dependence of the risk threshold  $E_{opt}$  on the moving speed  $v$ . The recovering rate  $\mu = 0.5$  and the contact radius  $r = 0.5$ .

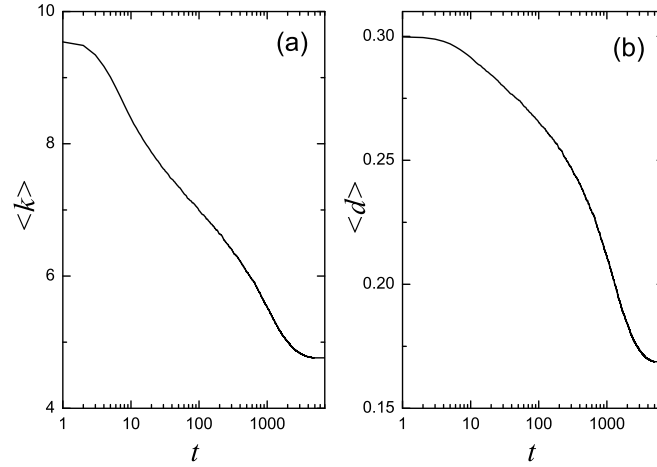


FIG. 3: (a) The average number of neighbors  $\langle k \rangle$  and (b) the average distance of two neighboring agents  $\langle d \rangle$ , as time  $t$  evolves. The spreading rate  $\lambda = 0.15$ , the recovering rate  $\mu = 0.4$ , the contact radius  $r = 0.45$ , the moving speed  $v = 0.3$ , and the risk threshold  $E = 7$ . Each curve is result of averaging over 100 random realizations.

A fundamental quantity in SIS dynamics is the epidemic threshold  $\lambda_c$ , below which the epidemic dies out. Due to the complexity of the model, it is very hard for us to obtain an analytical expression of  $\lambda_c$ . However, for large values of  $v$  and  $E = 0$ , the population is well mixed and the epidemic threshold can be given as:

$$\lambda_c = \frac{\mu}{\langle k \rangle} = \frac{\mu L^2}{\pi r^2 N}, \quad (3)$$

where  $\langle k \rangle$  denotes the average number of neighbors at each time step.

Figure 1 shows the dependence of  $\lambda_c$  on the risk threshold  $E$  for different values of the recovery rate  $\mu$ , the contact radius  $r$  and the moving speed  $v$ . From Fig. 1, one can see that for given values of other parameters, there exists an optimal value of  $E$ , hereafter denoted by  $E_{opt}$ , resulting in the maximum  $\lambda_c$ .

Figure 2 shows the risk threshold  $E_{opt}$  as a function of the recovering rate  $\mu$ , the contact radius  $r$  and the moving speed  $v$  respectively. For given values of other parameters,  $E_{opt}$  decreases from 8 to 7 as  $\mu$  increases from 0.1 to 1 [see Fig. 2(a)],  $E_{opt}$  increases from 4 to 10 as  $r$  increases from 0.3 to 0.6 [see Fig. 2(b)], and  $E_{opt}$  increases from 6 to 8 as  $v$  increases from 0.02 to 2 [see Fig. 2(c)].

For very large values of  $E$ , agents do no move and they have no chances to escape from the attack of infected neighbors. For very small values of  $E$  (e.g.,  $E = 0$ ), almost all agents move with the random directions, which cannot

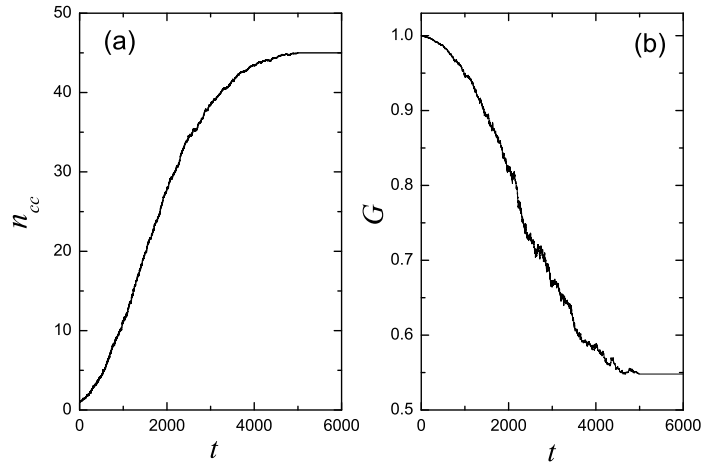


FIG. 4: (a) The number of connected components  $n_{cc}$  and (b) the normalized size of the largest component  $G$ , as time  $t$  evolves. The spreading rate  $\lambda = 0.15$ , the recovering rate  $\mu = 0.4$ , the contact radius  $r = 0.45$ , the moving speed  $v = 0.3$ , and the risk threshold  $E = 7$ . Each curve is result of averaging over 100 random realizations.

reduce the probability that encounters an infected agent. For the moderate value of  $E$ , agents will leave the heavily infected areas and stay at the slightly infected regions. An agent with more neighbors has higher probability of being infected and it tends to leave. On the other hand, an agent with less neighbors is more likely to stay at its current place as the number of infected neighbors is less than  $E$ . As a result, the average number of neighbors  $\langle k \rangle$  gradually decreases due to the migration driven by the moderate value of  $E$  [see Fig. 3(a)].

Counterintuitively, the decrease of the number of neighbors does not enlarge the distance between the two neighboring agents. From Fig. 3(b), we are surprising to find that the average distance of two neighboring agents  $\langle d \rangle$  decreases as time  $t$  evolves for the moderate value of  $E$ . This abnormal phenomenon indicates that agents are spontaneously divided into different components under the moderately risk-averse migration.

From the perspective of complex network theory, the topology of the system can be expressed as a dynamical network of mobile agents [20–24]. Every agent is regarded as a node of the network and a wireless link is established between two agents if their geographical distance is less than the contact radius  $r$ . Owing to the movement of agents, the network's structure changes with time. The decrease of the average number of neighbors and the average distance of two neighboring nodes indicates that agents are divided into different components under the moderately risk-averse migration. A component is a subgraph in which any two nodes are connected by a path. Note that each component is temporal as agents move with time.

Figure 4 shows the number of connected components  $n_{cc}$  and the normalized size of the largest component  $G$  as time  $t$  evolves when the risk threshold  $E$  is moderate. Initially, all agents form a connected component, corresponding to  $n_{cc} = 1$  and  $G = 1$ . As time evolves, the system is divided into more and more components [see Fig. 4(a)] and the size of the largest component decreases [see Fig. 4(b)].

Combining Figs. 3 and 4, we can understand why the epidemic spreading can be most inhibited by the moderately risk-averse migration. For non-migration ( $E$  is very large) and constant moving ( $E$  is very small), all agents construct a connected component and the average number of neighbors keep almost unchanged over time (the results are not shown here). For the moderate value of  $E$ , the formation of different components stop the epidemic spreading from one region to other regions. Moreover, for the moderately risk-averse migration, the average number of neighbors becomes smaller as time evolves, which greatly reduces the risk of being infected. Both of the above factors lead to the maximum epidemic threshold for the moderate value of  $E$ .

To intuitively understand how the moderate value of  $E$  affects the process of epidemic spreading, we plot the spatial distribution of susceptible and infected agents evolves with time when the spreading rate is a little smaller than the epidemic threshold. Initially, a small fraction of infected agents is randomly distributed [see Fig. 5(a)]. After a few time steps, the density of infected agents increases [see Fig. 5(b)]. However, with time the number of susceptible agents continually increases [see Fig. 5(c)] and finally they take over the whole system [see Fig. 5(d)]. Combining Figs. 5(a) and 5(d), one can observe that agents eventually aggregate to many different components in which they stay more closely than that in the initial state.

Finally, we investigate the effects of the recovery rate  $\mu$ , the contact radius  $r$  and the moving speed  $v$  on epidemic spreading. From Fig. 6(a), we see that for a given value of  $E$ , the epidemic threshold  $\lambda_c$  increases with  $\mu$ , which is

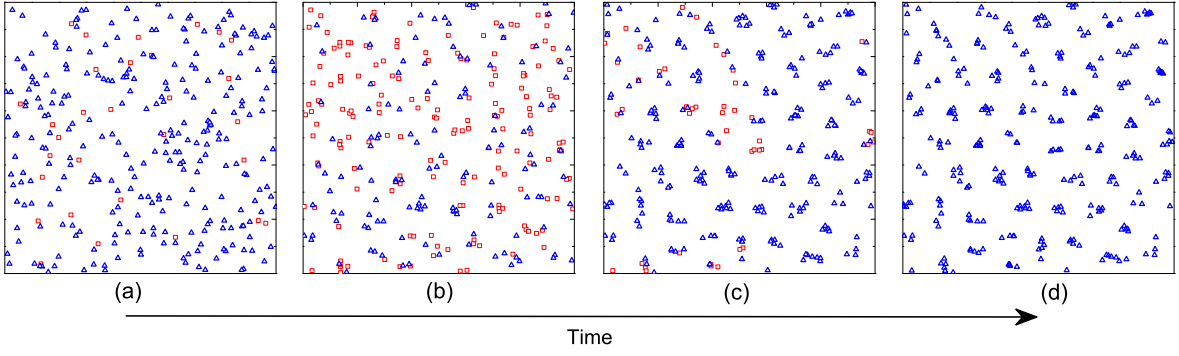


FIG. 5: (Color online) Snapshots of spatial distributions of susceptible agents (denoted by blue triangle) and infected agents (denoted by red square) at different time steps. The number of agents  $N = 300$ , the size of the square region  $L = 10$ , the spreading rate  $\lambda = 0.17$ , the recovering rate  $\mu = 0.4$ , the contact radius  $r = 1$ , the moving speed  $v = 0.3$ , and the risk threshold  $E = 7$ .

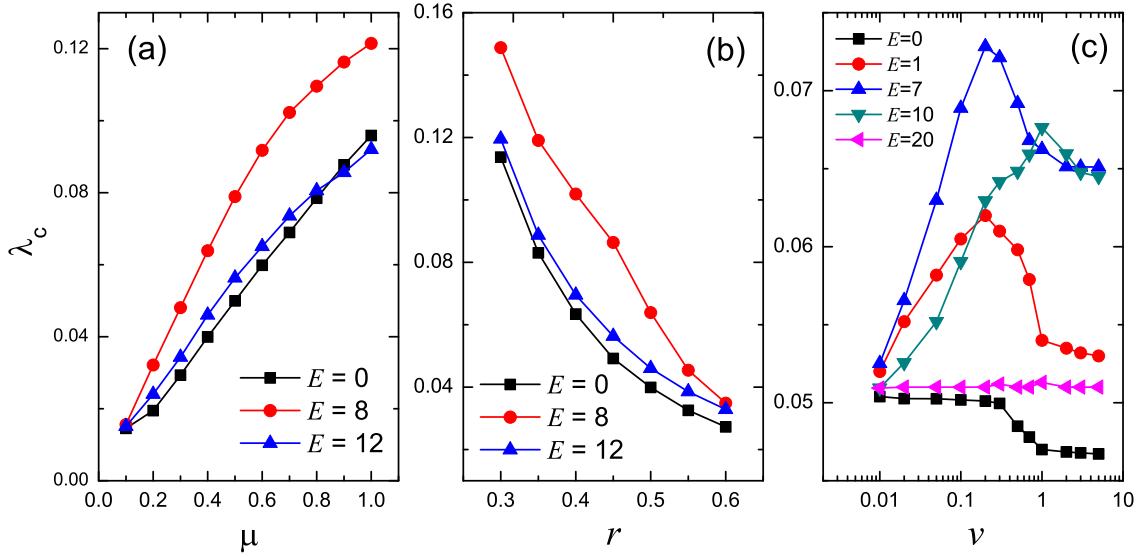


FIG. 6: (Color online) (a) The epidemic threshold  $\lambda_c$  as a function of the recovering rate  $\mu$  for different values of the risk threshold  $E$ . The contact radius  $r = 0.5$  and the moving speed  $v = 0.3$ . (b) The epidemic threshold  $\lambda_c$  as a function of the contact radius  $r$  for different values of  $E$ . The recovering rate  $\mu = 0.4$  and the moving speed  $v = 0.3$ . (c) The epidemic threshold  $\lambda_c$  as a function of the moving speed  $v$  for different values of  $E$ . The recovering rate  $\mu = 0.5$  and the contact radius  $r = 0.5$ . Each data point is result of averaging over 100 random realizations.

in accordance with previous studies [1]. The epidemic threshold  $\lambda_c$  decreases with  $r$  [see Fig. 6(b)]. In our model, the smaller value of  $r$  corresponds to the decrease of the neighbors. As is well known, the reduction in the number of the contacting neighbors effectively suppresses epidemic spreading, leading to a larger epidemic threshold [25]. From Fig. 6(c), one can see that the epidemic threshold  $\lambda_c$  decreases with  $v$  when  $E = 0$ . For very large values of  $E$  (e.g.,  $E = 20$ ), almost all agents do not move. In this case, the epidemic threshold does not change as the moving speed increases. For moderate values of  $E$ , the relation between  $\lambda_c$  and  $v$  is nonmonotonic, where an optimal value of  $v$  can maximize the epidemic threshold. From Fig. 6(c), one can also observe that the optimal value of  $v$  increases as  $E$  increases. For small values of  $v$ , agents move so slowly that the system is very close to the static network in which each agent's neighbors keep unchanged. For large values of  $v$ , agents move so fast that they cannot stay close to each other and cannot be divided into different components. Therefore, there must be an intermediate value of  $v$  that maximizes the epidemic threshold.

#### IV. CONCLUSIONS

To summarize, we have studied the effects of risk-averse migration on epidemic spreading. Each agent has the same contact radius  $r$ . Two agents can contact with each other if the geographical distance between them is less than  $r$ . An agent will move to a randomly chosen place with the speed  $v$  if the number of infected agents within its contact radius reaches or exceeds a risk threshold  $E$ . We find that the epidemic threshold can be maximized by an optimal value of  $E$ . For the moderate value of  $E$ , agents gradually form different components in which the average number of neighbors is much smaller than that for very small or very large value of  $E$ .

The interplay between information awareness and epidemic spreading in dynamical networks composed by mobile agents is an interesting research topic. Our findings presented here raise a number of open questions, answers to which could further deepen our understanding of the role of migration in epidemic spreading. For example, what happens if the contact radius or the moving speed is not the same for all agents? Another interesting issue is whether agents can move with the preferential directions rather than the random directions? In the present work, an individual determinately leaves if the number of infected neighbors reaches or exceeds  $E$ . What would happen if an individual leaves with some probability?

#### Acknowledgments

This work was supported by the National Science Foundation of China (Grants No. 61403083, No. 71301028 and No. 11575041).

- 
- [1] Pastor-Satorras R, Castellano C, Mieghem PV, Vespignani A. Epidemic processes in complex networks. *Rev Mod Phys.* 2015; 87: 925-979.
  - [2] Wang Z, Bauch CT, Bhattacharyya S, d'Onofrio A, Manfredi P, Perc M, Perra N, Salathé M, Zhao D. Statistical physics of vaccination. *Phys Rep.* 2016; 664: 1-113.
  - [3] Wang Z, Andrews MA, Wu ZX, Wang L, Bauch CT. *Phys Life Rev.* Coupled disease-behavior dynamics on complex networks: A review. 2015; 15: 1-29.
  - [4] Funk S, Gilad E, Jansen V. Endemic disease, awareness, and local behavioural response. *J Theor Biol.* 2010; 264: 501-509.
  - [5] Meloni S, Perra N, Arenas A, Gómez S, Moreno Y, Vespignani A. Modeling human mobility responses to the large-scale spreading of infectious diseases. *Sci Rep.* 2011; 1: 62.
  - [6] Ruan Z, Tang M, Liu Z. Epidemic spreading driven by information-driven vaccination. *Phys Rev E.* 2012; 86: 036117.
  - [7] Cardillo A, Reyes-Suárez C, Naranjo F, Gómez-Gardeñes J. Evolutionary vaccination dilemma in complex networks. *Phys Rev E.* 2013; 88: 032803.
  - [8] Granell C, Gómez S, Arenas A. Competing spreading processes on multiplex networks: awareness and epidemics. *Phys Rev E.* 2014; 90: 012808.
  - [9] Sanz J, Xia CY, Meloni S, Moreno Y. Dynamics of interacting diseases. *Phys Rev X.* 2014; 4: 041005.
  - [10] Cai CR, Wu Z, Guan JY. Effect of vaccination strategies on the dynamic behavior of epidemic spreading and vaccine coverage. *Chaos Solition Fract.* 2014; 62-63: 36-43.
  - [11] Pu C, Li S, Yang J. Epidemic spreading driven by biased random walks. *Physica A.* 2014; 432: 230-239.
  - [12] Shen Z, Cao S, Wang WX, Di Z, Stanley HE. Locating the source of diffusion in complex networks by time-reversal backward spreading. *Phys Rev E.* 2016; 93: 032301.
  - [13] Gross T, D'Lima CJD, Blasius B. Epidemic dynamics on an adaptive network. *Phys Rev Lett.* 2006; 96: 208701.
  - [14] Funk S, Gilad E, Watkins C, Jansen VA. The Spread of Awareness and Its Impact on Epidemic Outbreaks. *Proc Natl Acad Sci U S A.* 2009; 106: 6872-6877.
  - [15] Granell C., Gómez S, Arenas A. Dynamical interplay between awareness and epidemic spreading in multiplex networks. *Phys Rev Lett.* 2013; 111: 128701.
  - [16] Wang W, Tang M, Yang H, Do Y, Lai YC, Lee G. Asymmetrically interacting spreading dynamics on complex layered networks. *Sci Rep.* 2014; 4: 5097.
  - [17] Xia CY, Wang L, S Sun, J Wang. An SIR model with infection delay and propagation vector in complex networks. *Nonlinear Dynamics.* 2012; 69: 927-934.
  - [18] Xia CY, Wang Z, Sanz J, Meloni S, Moreno Y. Effects of delayed recovery and nonuniform transmission on the spreading of diseases in complex networks. *Physica A.* 2013; 392: 1577-1585.
  - [19] Gao Y, Du WB, Yan G. Selectively-informed particle swarm optimization. *Sci Rep* 2015; 5: 9295.
  - [20] Du WB, Gao Y, Liu C, Zheng Z. Adequate is better: particle swarm optimization with limited-information. *Appl Math Comput.* 2015; 268: 832-838.
  - [21] Chen MH, Wang L, Wang J, Sun SW, Xia CY. Impact of individual response strategy on the spatial public goods game within mobile agents. *Appl. Math. Comput.* 2015; 251: 192-20

- [22] Du WB, Zhou XL, Lordan O, Wang Z, Chen Z, Zhu YB. Analysis of the Chinese Airline Network as multi-layer networks. *Transport Res E*. 2016; 89: 108-116.
- [23] Du WB, Liang BY, Yan G, Lordan O, Cao XB. Identifying vital edges in Chinese air route network via memetic algorithm. *Chinese Journal of Aeronautics*. 2017; 30: 330-336.
- [24] Yang X, Li J, Pu C, Yan M, Sharafat RR, Yang J, Gakis K, Pardalos PM. Traffic congestion and the lifetime of networks with moving nodes. *Phys Rev E*. 2017; 95: 012322.
- [25] Pastor-Satorras R, Vespignani A. Epidemic dynamics in finite size scale-free networks. *Phys Rev E*. 2002; 65: 035108.